

## Article

# Development and Analysis of Solutions to Improve the Efficiency of Volute Inlet Pipes in Radial Turboexpanders

Sergey Osipov <sup>1</sup>, Nikolay Rogalev <sup>2</sup>, Andrey Rogalev <sup>1</sup>, Ivan Komarov <sup>1</sup> and Dmitriy Lvov <sup>1,\*</sup>

<sup>1</sup> Department of Innovative Technologies of High-Tech Industries, Moscow Power Engineering Institute National Research University, 111250 Moscow, Russia

<sup>2</sup> Department of Thermal Power Plants, Moscow Power Engineering Institute, National Research University, Krasnokazarmennaya St. 14, 111250 Moscow, Russia

\* Correspondence: lvovdd@mpei.ru

**Abstract:** The annual increase in demand for electrical power is accompanied by a significant combustion of hydrocarbon fuels and, accordingly, significant CO<sub>2</sub> emissions into the atmosphere, which, in turn, result in increasing the surface temperature of our planet. In addition, hydrocarbon fuel reserves are also depleted every year, which raises the question of the efficient use of fossil fuels. One of the promising solutions to this problem is introducing a technology that allows using the excess gas pressure at gas distribution points in order to generate additional electrical energy. As a rule, a radial turboexpander is used to convert the kinetic energy of natural gas at low power. In this paper, we study a method to reduce losses in a volute inlet of a radial expander. Based on our research, we could find that the use of two symmetrical fins in the volute inlet pipe makes it possible to decrease the turbulent kinetic energy by 1.29% and to reduce the energy losses in the inlet pipe by 2.18%.



**Citation:** Osipov, S.; Rogalev, N.; Rogalev, A.; Komarov, I.; Lvov, D. Development and Analysis of Solutions to Improve the Efficiency of Volute Inlet Pipes in Radial Turboexpanders. *Inventions* **2022**, *7*, 124. <https://doi.org/10.3390/inventions7040124>

Academic Editor: Amjad Anvari-Moghaddam

Received: 18 November 2022

Accepted: 6 December 2022

Published: 13 December 2022

**Publisher's Note:** MDPI stays neutral with regard to jurisdictional claims in published maps and institutional affiliations.



**Copyright:** © 2022 by the authors. Licensee MDPI, Basel, Switzerland. This article is an open access article distributed under the terms and conditions of the Creative Commons Attribution (CC BY) license (<https://creativecommons.org/licenses/by/4.0/>).

**Keywords:** radial turboexpander; natural gas; volute inlet pipe; gas-dynamic efficiency

## 1. Introduction

Natural gas occupies a special place among all known fuels. The main advantage of gas, as compared to solid and liquid fuels, is its good environmental performance, in addition to a high calorific value. The absence of slag and ash in the exhaust gases allows for using gas fuel for household needs, at thermal power plants, in house boiler, and at industrial enterprises. This explains the large volumes of gas production and the need to transport it to consumers [1,2].

Currently, there is an urgent problem of inefficient use of the excess pressure of natural gas in the energy sector, in industrial production, and in housing maintenance services. At most natural gas depressurization points of the Russian gas transmission network, its potential energy is irretrievably lost due to the gas expansion to a pressure required by its consumers. At the moment, there are more than five hundred gas distribution stations (GDS) in Russia and a much larger number of gas pressure regulation stations (GPRS), where gas is irretrievably expanded. The existing system of natural gas transportation from its production facilities to the consumers makes it possible to provide an additional electrical power generation at pressure reduction service stations using recycled turboexpander systems [3].

The main structural elements of the flow path of a radial expander are a volute inlet pipe, nozzle guide vanes, a radial wheel, and an outlet pipe. An important task when designing this class of turbomachines is creating an unseparated flow of the working medium both in inter-blade channels of the turbine stages and in the inlet and outlet pipes. The presence of separation in the turbomachine flow path decreases its efficiency (because of additional energy losses) and reliability (because of increased vibration). Currently, there

is an urgent issue of developing simple and effective flow control methods that allow to reduce the vortex formation in structural elements of radial turboexpanders [4,5].

The flow structure upstream of the inter-blade channels of the flow path of a radial turboexpander depends on the flow structure in the inlet pipe. The inlet pipe shape of a radial turbine is a convergent convoluted channel. An important drawback of the volute inlet pipe is the formation of a vortex motion, which is a source of secondary losses, the proportion of which is of the same order as the profile-related losses [6].

There are known studies [7,8] whose authors explore the effect of changing the tongue angle with its constant and variable radii in terms of the strength characteristics and the gas-dynamic efficiency of the volute inlet pipe of a radial turbomachine. For the turbine to operate with of the maximum efficiency, the researchers suggest using a configuration with a small radius of the tongue and its inclination angle; in case where it is necessary to improve the turbine reliability and to minimize the risk of the wheel blade fatigue failure, they suggest using a high tongue angle configuration.

There is also a known study [9] where the authors consider the effect of the square and elliptical tongue shapes on the service life of a radial turbomachine. The use of an elliptical tongue reduces the plastic deformation by 74% from 0.66 to 0.17%, as compared to the square design.

In addition, there is the study [10], which investigates the effect of changing the radial clearance between the impeller and the volute inlet pipe tongue of a radial turbomachine. The authors of this study made the following conclusions: increasing the radial clearance from 0.067D2 to 0.224D2 reduces the pressure pulsation two times on average along the entire path of a volute inlet pipe.

A similar research for blower systems was carried out in [11]. The findings of this study have no quantitative assessment; but qualitatively, they coincide in many respects with [10]. As the radial clearance between the impeller and volute inlet pipe tongue increased, the pressure decreases, and the efficiency increases. These results confirm that the radial clearance between the impeller and volute inlet pipe tongue affects the machine's performance.

The paper [12] presents the results of the study of an asymmetric two-way radial turbomachine. The result of this study is the following recommendation when designing this type of machines: in case where a manifold with a large flow area is required, it is advisable to install the large spiral on the casing side, which will increase the gas-dynamic efficiency of the entire machine by 1.6%. When a manifold with a small flow section area is required, it is better to install the large spiral on the hub side, which will increase the gas-dynamic efficiency of the entire machine by 1.1%.

We also know the study [13] where the authors solve the problem of uneven distribution of the working medium in the flow path of a volute inlet pipe when cooling the impeller rear disk. It was found that changing the entry angle of the working medium into the volute inlet pipe could reduce the uneven cooling efficiency by 26.2%.

The results of gas-dynamic studies of the flow structure in the inlet pipe of a radial turboexpander have shown that one of the ways to improve the inlet pipes of radial turbines is decreasing the intensity of secondary flows. The authors of study [14] suggest using a longitudinal fin to decrease the intensity of secondary flows and, accordingly, to reduce the energy losses in a volute inlet pipe. The fin length must be of 90 to 270° (mainly, 100 to 180°) of the inlet pipe involute, and the height must be of 0.3 to 0.5 (mainly, 0.5) of the meridional section diameters of the spiral chamber. It should be noted that the authors provided only a qualitative description of this effect without mentioning its quantitative indicators.

We should note that it is possible to reduce the energy losses in a volute inlet pipe by using special fins for decreasing the intensity of secondary flows, only if additional losses from friction on the fin surface are less than the decrease in energy losses due to the existence of vortex structures in the channel.

## 2. Materials and Methods

The Materials and Methods should be described with sufficient details to allow others in this paper, we have considered various design configurations of a volute inlet pipe, the geometrical parameters of which are shown in Figure 1, namely [15]:

- Without fins;
- Longitudinal flat fin (type 1);
- Two symmetrical flat fins (type 2);
- Two symmetrical rounded fins (type 3);
- Two symmetrical short fins in the flow (type 4).

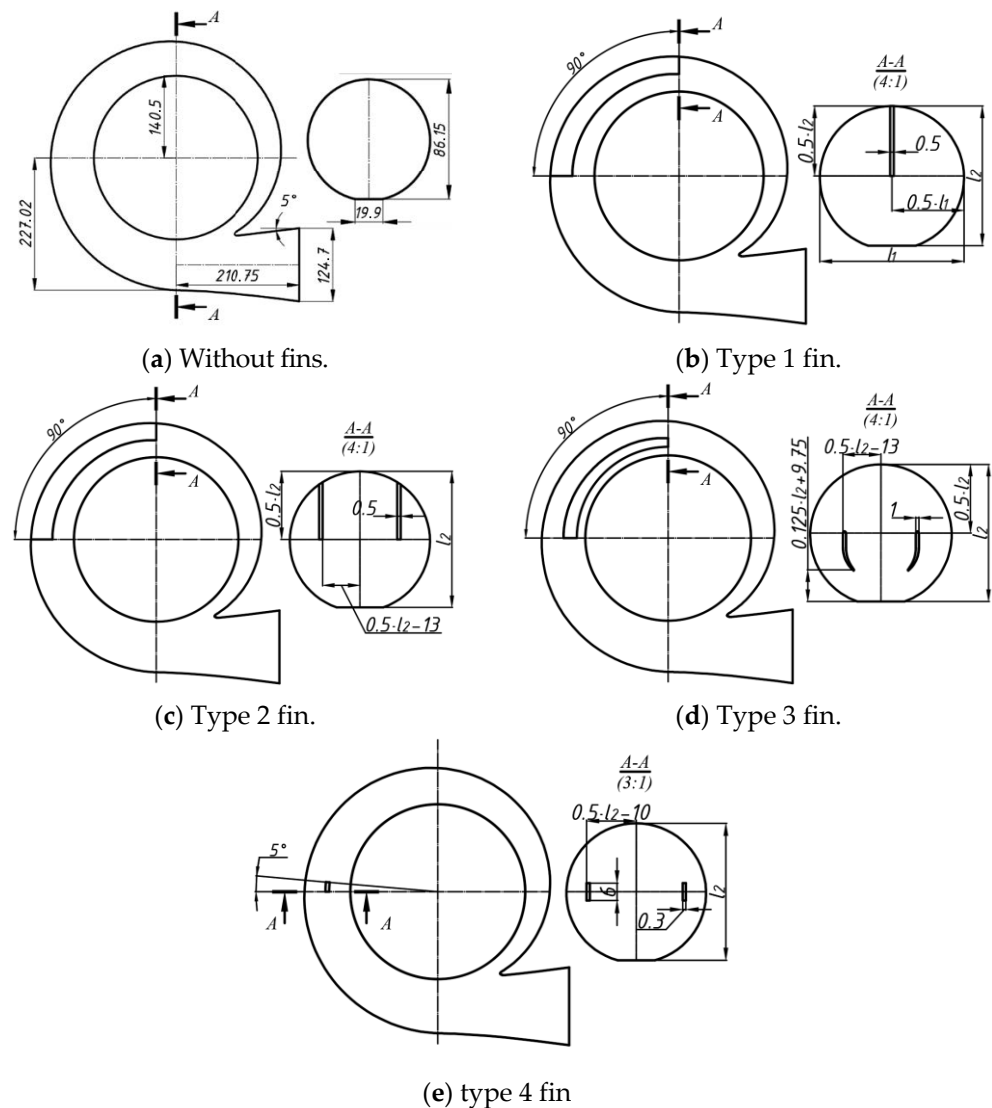


**Figure 1.** Schemes of the investigated inlet pipes of a low power turboexpander.

As the research method, we have selected the simulation by Reynolds averaging of the Navier–Stokes equation system (RANS). The computational grid for the volume of the inlet pipe flow path is hybrid and unstructured. The main flow area was built of tetrahedra, and the near-wall layer area was built of prisms. The computational grid parameters did not depend on the inlet pipe shape and remained constant for all variants of the research.

The computational grid parameters for simulating the flow were determined to obtain adequate results when using the turbulence SST model. This model was chosen due to the fact that with this geometry of the object, it is assumed that there is a flow separation in the boundary layer, which in turn excludes the possibility of using the k-ε model, since it

does not allow an adequate assessment of the flow behavior in this case [16]. The selected computational grid parameters for the inlet pipe are given in Table 1.

**Table 1.** Computational grid parameters for the flow volume.

Parameter	Value
Maximum linear size of an element, mm	1.8
Number of prism layers, units	15
$y^+$	5
Height of the first prism layer, mm	0.01021
Ratio of the heights of neighboring prisms	1.2
Total height of prism layers, mm	0.88039
Growth pattern	wb–exponential

The choice of parameters for modeling largely depends on the global grid cell size. Performing calculations for various sizes of the global element, it was found that with allowable restrictions of less than 1.8 mm, the error in determining the losses is less than 1%, but it eludes the calculation time. Figure 2 shows the grid convergence plot.

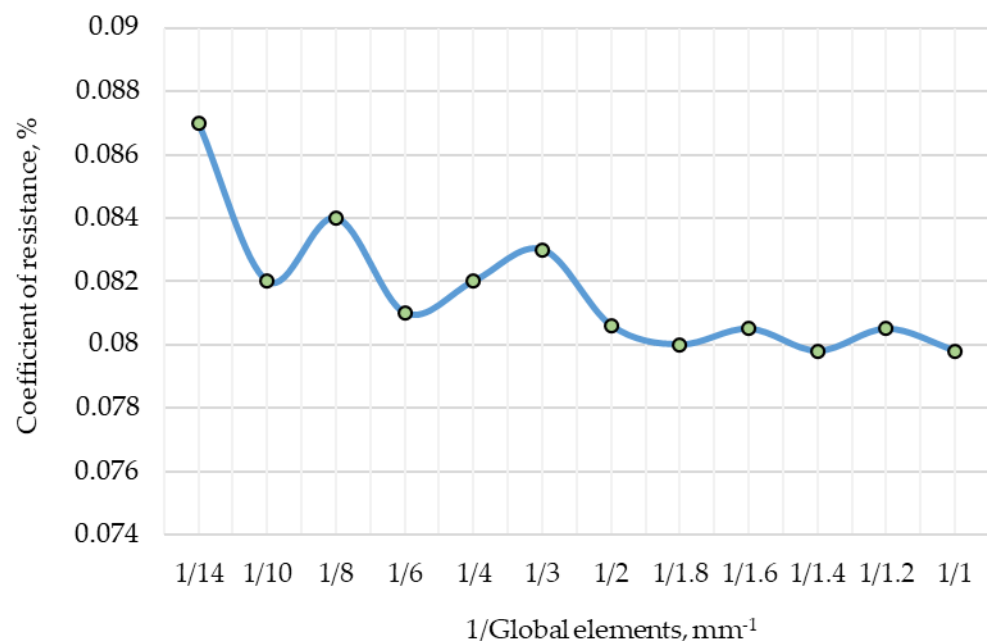


**Figure 2.** Grid convergence.

For illustration purposes, Figure 3 shows computational grids for various inlet pipes. The total size of the computational grid varied within a range of 8.89 to 10.28 million elements, depending on the volute shape.

Our gas-dynamic studies of the flow structure in inlet pipes of a low-power turboexpander were carried out using the method of Reynolds averaging the Navier–Stokes equations in the Ansys CFX software module. The boundary conditions under which the digital simulation was carried out were assumed to be the same for all inlet pipe variants. The boundary conditions are shown in Figure 4 using the example of a round symmetrical inlet pipe.

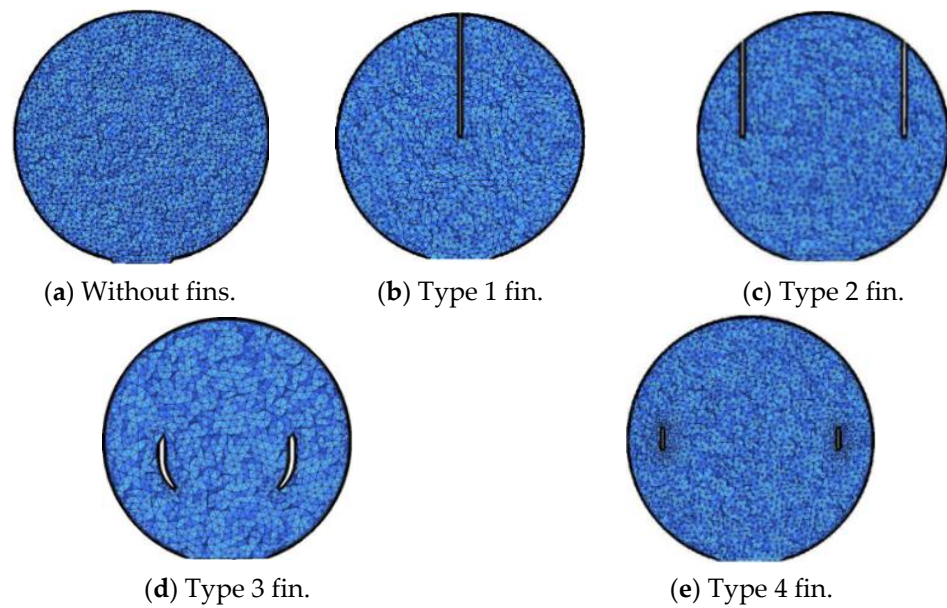


Figure 3. Computational grid for the flow.

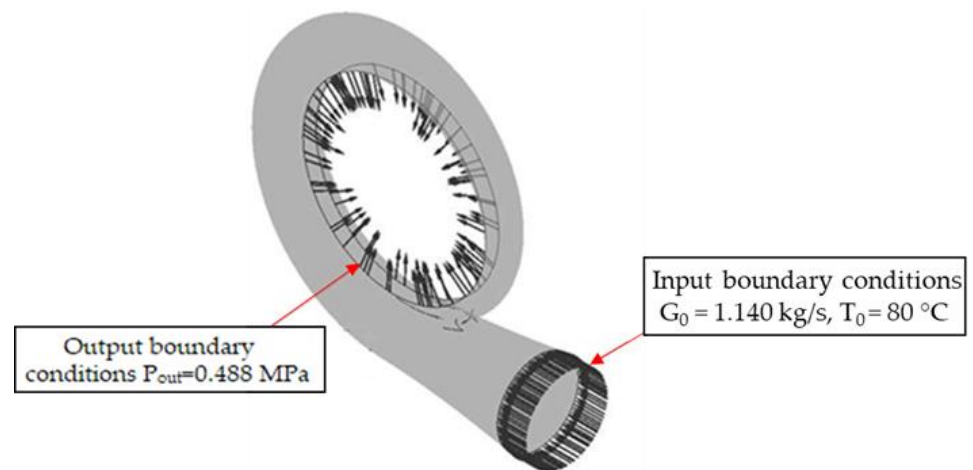


Figure 4. Boundary conditions of the model.

Upstream of the inlet pipe, the flow rate of natural gas  $G_0$  was set to be equal to 1.140 kg/s, and the stagnation temperature  $T_0$  equal to 80 °C. A constant static pressure  $P_{st}$  at the outlet of the channel was obtained from a one-dimensional calculation of the flow and was set as equal to 0.48859 MPa.

The calculation of the coefficient of hydraulic resistance was carried out according to the mixture of the formula presented in the work [17].

$$\zeta = \zeta_f + \zeta_{local} = \frac{2 \cdot \Delta P}{\rho \cdot w^2}, \tag{1}$$

where  $\zeta_f$  is the coefficient of friction loss;  $\zeta_{local}$  is the coefficient of local resistance;  $\Delta P$  is the pressure difference at the inlet and outlet of the volute, Pa;  $\rho$  is the average density of work substance, kg/m<sup>3</sup>;  $w$  is the average velocity in longitudinal section, m/s.

The coefficient of friction loss was determined by the formula:

$$\zeta_f = C_f \frac{L}{b}, \tag{2}$$

where  $C_f$  is the coefficient of frictional resistance units of the relative length of the section;  $L$  is the length of the rib, m;  $b$  is the width of the rib, m.

The coefficient of friction resistance of a unit of relative length of the section, in turn, is determined by the formula presented in the work [18].

$$C_f = \frac{0.059}{(Re_x)^{\frac{1}{5}}} = \frac{0.059}{\left(\frac{w \cdot L}{\nu}\right)^{\frac{1}{5}}}, \tag{3}$$

### 3. Results and Discussion

To obtain the most accurate results, we should consider the flow parameters distribution in eight different radial sections of the volute (Figure 5).

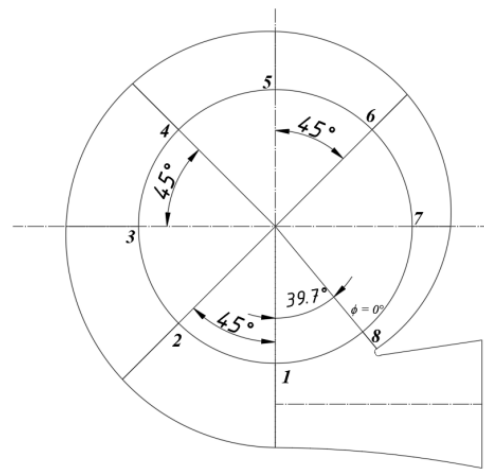


Figure 5. Radial sections of a volute inlet pipe.

Our analysis of the full pressure and velocity distribution, as shown in Figures 6 and 7, in longitudinal sections of the inlet pipe with various fin types has demonstrated that the changes are insignificant, as compared to a volute without fins. In the inlet pipe with a flat fin, an edge mark appears in the center of the volute, which occurs due to the separation of the flow from the fin, as a result of which the pressure and velocity of the flow core in the area where the fin is installed is reduced. This phenomenon, in turn, leads to an increase in the non-uniformity of the flow and additional energy losses associated with its equalization.

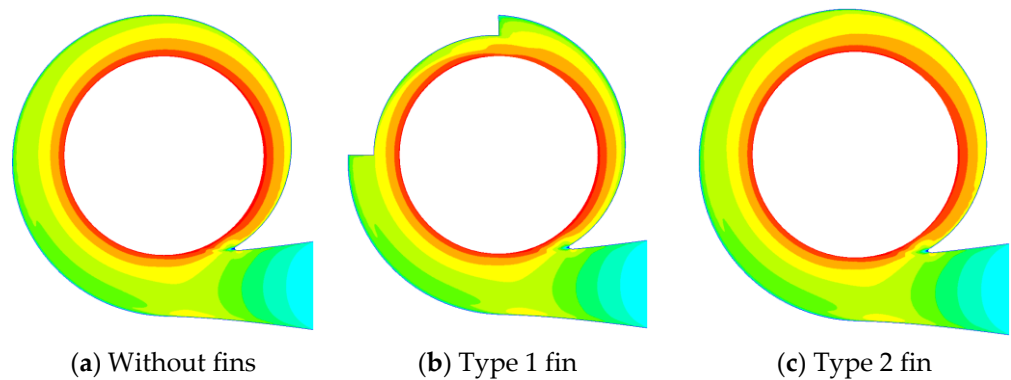


Figure 6. Cont.

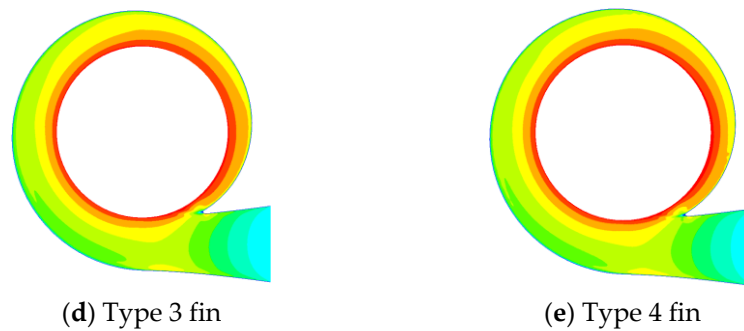


Figure 6. Velocity field in the central longitudinal section of the inlet pipe.

The full pressure plots and the flow line structure from the first radial section ( $39.7^\circ$ ) to the third one ( $129.7^\circ$ ) are virtually identical in all variants considered. Starting from the third section ( $129.7^\circ$ ), the full pressure distribution depends on the fin type. Installing a fin №1 results in the emergence of an edge trail and an increased radial and edge unevenness. The resistance coefficient of an inlet pipe with fin №1 is 10.2% higher than the resistance coefficient of an inlet pipe without fins. The turbulence kinetic energy in the fourth and fifth (from  $174.7$  to  $219.7^\circ$ ) radial sections of the inlet pipe with a fin is higher by 13 and 17%, respectively. Therefore, installing a longitudinal flat fin in the center of a volute inlet pipe does not provide any positive effect (type 1). Our analysis of the flow line structures, as shown in Figure 7, in inlet pipes with two symmetrical fins (type 2) has demonstrated that installing two fins, as well as installing a single longitudinal fin, does not eliminate the vortex formation from the third ( $129.7^\circ$ ) to the fifth ( $219.7^\circ$ ) radial sections. The resistance coefficient of an inlet pipe with fin №2 is 14.8% higher than the resistance coefficient of an inlet pipe without fins. Using two symmetrical rounded fins (type 3) allows virtual elimination of the paired vortices and to stabilize the flow. However, the resistance coefficient of an inlet pipe with fin №3 is 15% higher than the resistance coefficient of an inlet pipe without fins. Using two symmetrical short fins in the flow (type 4) does not eliminate the vortex formation, as shown in Figures 8 and 9, from the third ( $129.7^\circ$ ) to the fourth ( $174.7^\circ$ ) sections. However, starting from the fifth ( $219.7^\circ$ ) section, vortices are virtually absent. In all cases, the use of fins improves the flow evenness starting from the sixth radial section ( $264.7^\circ$ ). The qualitative assessment of the vortex structure in the third and fifth sections allows us to conclude that the least vortex formation is achieved in the inlet pipe with two symmetrical short fins in the flow (type 4).

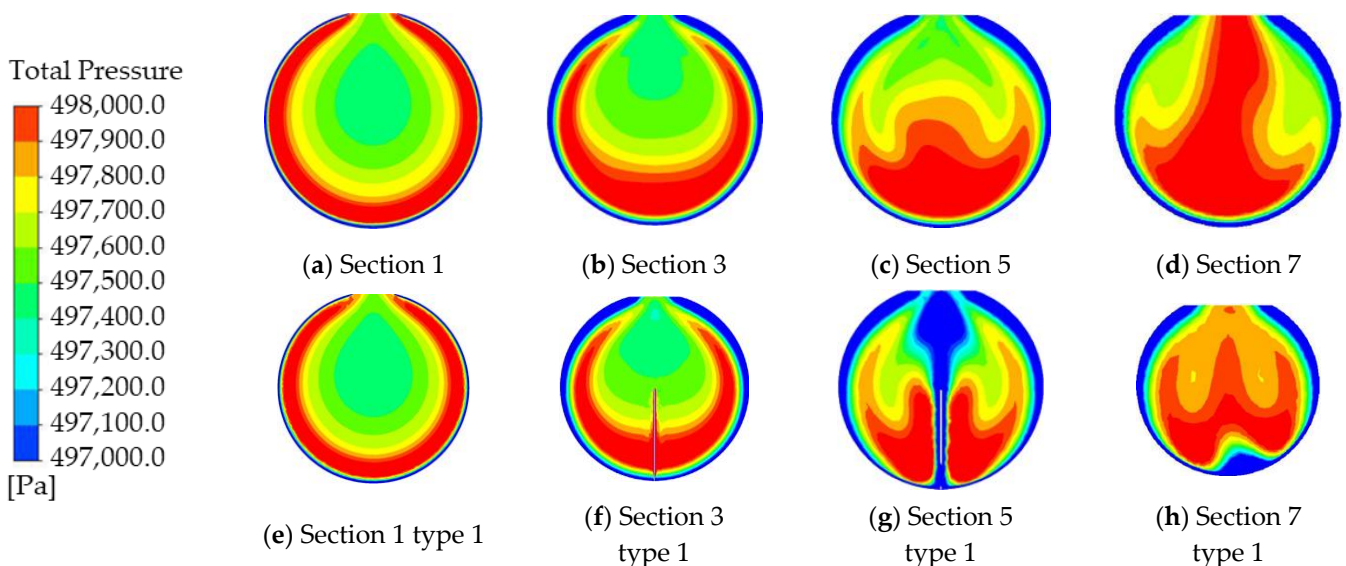


Figure 7. Cont.

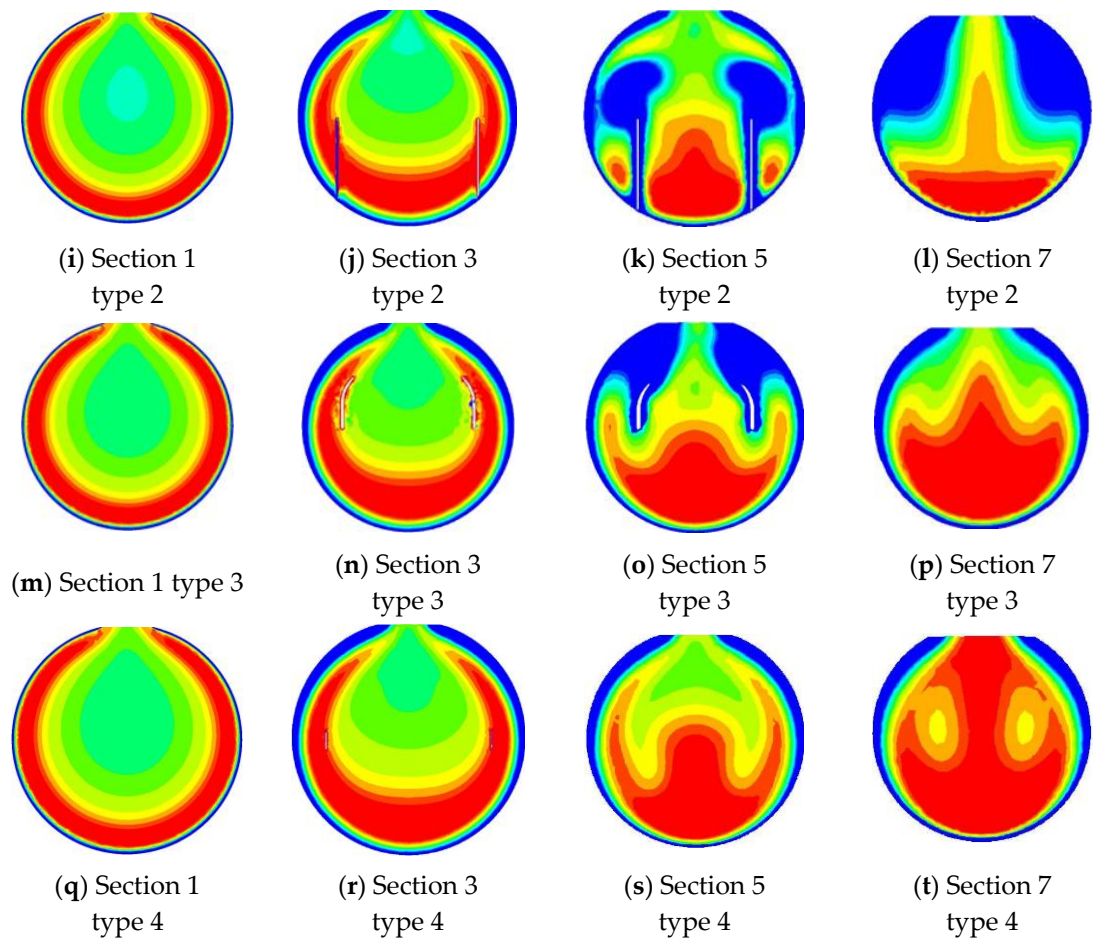


Figure 7. Distribution of the pressure field in the inlet pipe with various fin types.

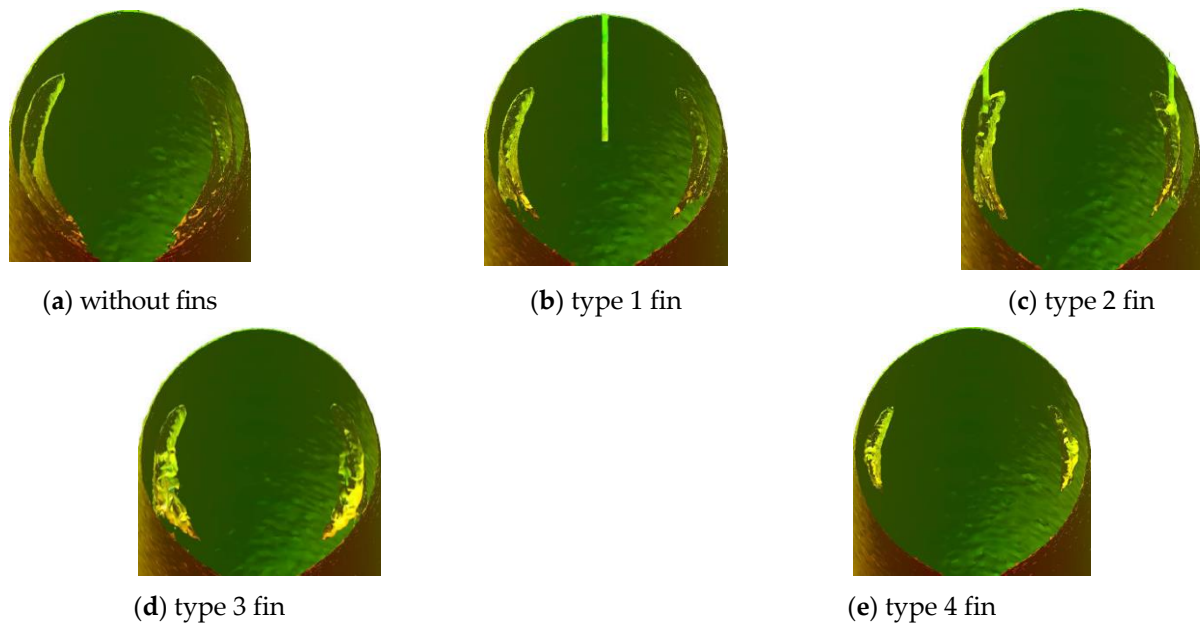
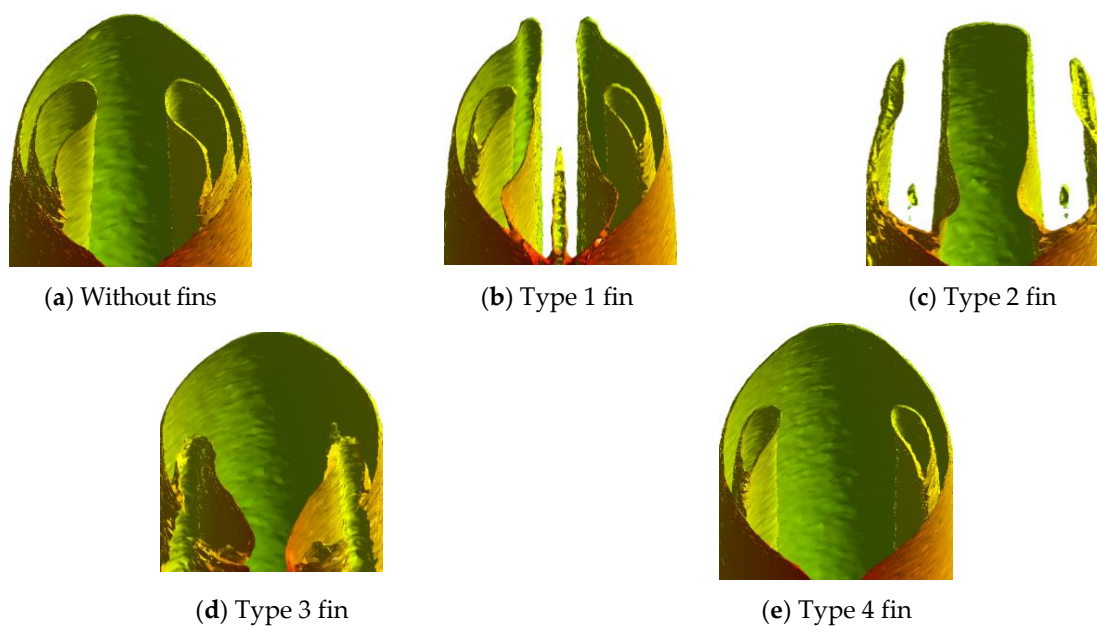


Figure 8. Vortex formation in section 3 of an inlet pipe.



**Figure 9.** Vortex formation in section 5 of an inlet pipe.

Tables 2 and 3 present the results of calculating the coefficient friction and resistance using the methods described in [17] for an inlet pipe with various fin types, whereas Figures 10 and 11 show the composition of hydraulic resistance losses when using different types of fins and the distribution of the turbulence kinetic energy along the volute. The minimum resistance coefficient is equal to 0.07857 for an inlet pipe with fin type 4. When using this type of fin, the resistance coefficient is reduced by 2.18% as compared to an inlet pipe without fins. Analysis of the resistance coefficient shows that the installation of ribs of type No. 1, 2, and 3 allows to reduce the loss from eddies, respectively, by 18.9, 53.4, and 49.0%; however, the loss from sets that are, respectively, 26.4, 59.2, 55.5, and 46.3% of the resistance coefficient, has a greater effect on pressure increase than the effect of reducing vortex formation. The distribution of the turbulence kinetic energy in the inlet pipe also shows that the least value is that of a volute with two short symmetrical fins in the flow (type 4). In inlet pipes with other fin types, the turbulence kinetic energy is significantly higher from 130 to 220°.

**Table 2.** Friction coefficient as calculated.

Name	w, m/s	L, m	b, m	v, m <sup>2</sup> /s	C <sub>f</sub>	ξ <sub>f</sub>
Type 1 fin	78.84	0.377	0.043	1.5 × 10 <sup>-6</sup>	2.048 × 10 <sup>-3</sup>	0.017
Type 2 fin	78.64	0.377	0.037	1.5 × 10 <sup>-6</sup>	2.049 × 10 <sup>-3</sup>	0.041
Type 3 fin	78.75	0.27	0.03	1.5 × 10 <sup>-6</sup>	2.191 × 10 <sup>-3</sup>	0.039
Type 4 fin	79.65	0.0235	0.006	1.5 × 10 <sup>-6</sup>	3.561 × 10 <sup>-3</sup>	0.027

**Table 3.** Resistance coefficient as calculated.

Name	ΔP, Pa	w, m/s	ρ, kg/m <sup>3</sup>	ξ
No fins	678	79.37	2.680	0.080
Type 1 fin	737	78.84	2.680	0.088
Type 2 fin	760	78.64	2.680	0.091
Type 3 fin	768	78.75	2.680	0.092
Type 4 fin	668	79.65	2.680	0.078

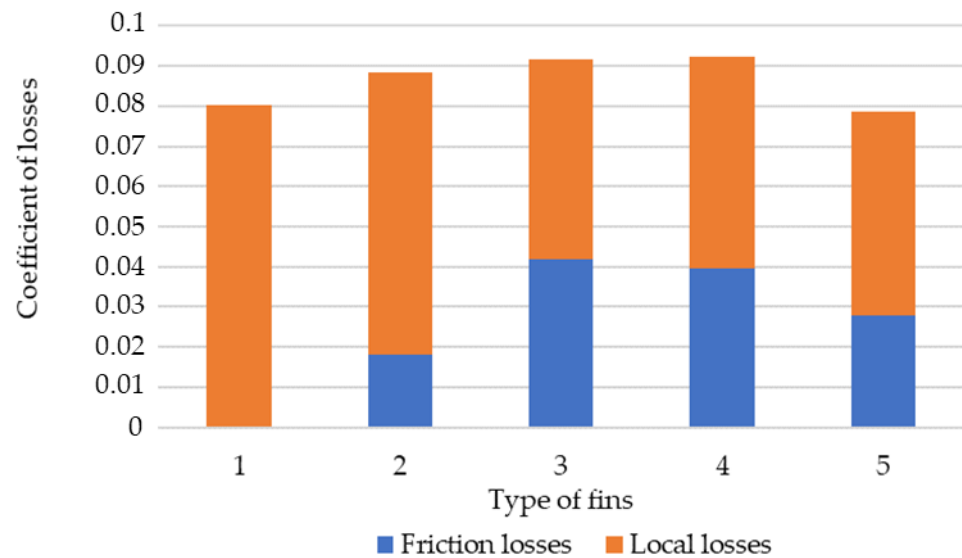


Figure 10. The composition of hydraulic resistance losses when using different types of fins.

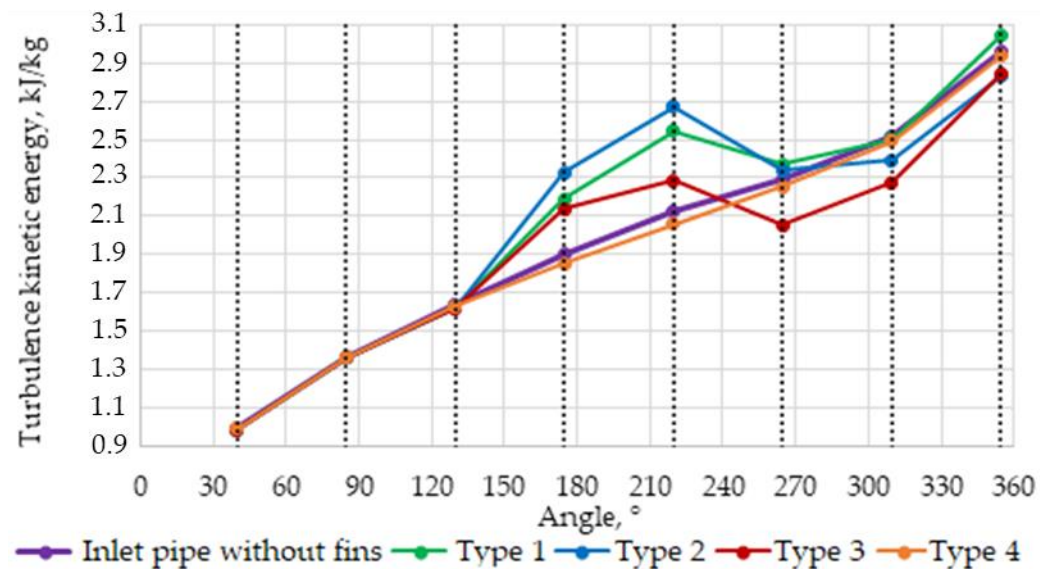


Figure 11. Distribution of the turbulence kinetic energy in inlet pipes with various fin types.

#### 4. Conclusions

In this paper, it was numerically established that the use of a fin No. 1 does not lead to a positive effect. The coefficient of resistance in this case is 9.2% higher than in the version without fins, due to the appearance of an edge trace and an increase in radial and circumferential unevenness. In addition, the use of fins No. 2 and No. 3 also leads to an increase in the coefficient of resistance. Despite the fact that there is a leveling of the flow and a decrease in vortex formation in the flowing part of the snail pipe, friction losses have then a predominant share compared to the positive effect.

However, it is possible to reduce the energy losses associated with the presence of vortex structures in the supply snail pipe of the turboexpander by installing two symmetrically arranged rectangular cross-section ribs located at the average radius of the meridional section. The use of these two intermediate fins No. 4 in the supply snail nozzle allows to reduce turbulent kinetic energy by 1.29% and reduce energy losses in the nozzle by 2.18% at the nominal operating mode of a low-power radial turboexpander.

**Author Contributions:** Conceptualization, S.O. and N.R.; methodology, A.R. and I.K.; software, S.O. and D.L.; validation, S.O. and I.K.; formal analysis, N.R. and A.R.; investigation, I.K. and S.O.; resources, A.R. and I.K.; data curation, I.K. and S.O.; writing (original draft preparation), D.L.; writing (review and editing), D.L. and S.O.; visualization, D.L.; supervision, N.R.; project administration, I.K. and A.R.; funding acquisition, I.K. and A.R. All authors have read and agreed to the published version of the manuscript.

**Funding:** This study conducted by the Moscow Power Engineering Institute was financially supported by the Ministry of Science and Higher Education of the Russian Federation (project no. FSWF-2020-0020).

**Data Availability Statement:** Not applicable.

**Conflicts of Interest:** The authors declare no conflict of interest.

## References

1. Protalinsky, O.M.; Shcherbatov, I.A.; Stepanov, P.V. Identification of the Actual State and Entity Availability Forecasting in Power Engineering Using Neural-Network Technologies. In Proceedings of the International Conference “Problems of Thermal Physics and Power Engineering” (PTPPE-2017), Moscow, Russia, 9–11 October 2017; Volume 891, p. 12289.
2. Arakelian, E.; Shcherbatov, I.; Tsurikov, G.; Titov, F.; Pashchenko, A. Creation of Predictive Analytics System for Power Energy Objects. In Proceedings of the 2019 Twelfth International Conference “Management of Large-Scale System Development” (MLSD), Moscow, Russia, 1–3 October 2019; pp. 1–5.
3. Osipov, S.; Zonov, A.; Makhmutov, B.; Zaryankin, A. Circulating Water Cooling System Using a Turbo-Expander at Gas Thermal Power Plants. *AIP Conf. Proc.* **2019**, *2189*, 20017.
4. Zaryankin, A.; Rogalev, A.; Kindra, V.; Khudyakova, V.; Bychkov, N. Reduction Methods of Secondary Flow Losses in Stator Blades: Numerical and Experimental Study. In Proceedings of the 12th European Conference on Turbomachinery Fluid Dynamics & Thermodynam, Stockholm, Sweden, 3–7 April 2017; p. 11.
5. Zaryankin, A.; Rogalev, A.; Komarov, I.; Kindra, V.; Osipov, S. The Boundary Layer Separation from Streamlined Surfaces and New Ways of its Prevention in Diffusers. In Proceedings of the 12th European Conference on Turbomachinery Fluid Dynamics & Thermodynamics, Stockholm, Sweden, 3–7 April 2017.
6. Rogalev, A.; Rogalev, N.; Komarov, I.; Kindra, V.; Osipov, S. Methods for Competitiveness Improvement of High-Temperature Steam Turbine Power Plants. *Inventions* **2022**, *7*, 44. [[CrossRef](#)]
7. Rodgers, C.; Geiser, R. Performance of a high-efficiency radial/axial turbine. *ASME J. Turbomach.* **1987**, *109*, 151–154. [[CrossRef](#)]
8. Suhrmann, J.F.; Peitsch, D.; Gugau, M.; Heuer, T. On the effect of volute tongue design on radial turbine performance. *Turbo Expo Power Land Sea Air. Am. Soc. Mech. Eng.* **2012**, *44748*, 891–901.
9. Suhrmann, J.F.; Peitsch, D.; Gugau, M.; Heuer, T. Development of Models for Optimum Wheel Flow Inlet Angles of Small Size Radial Turbines. In Proceedings of the 10th International Gas Turbine Congress (IGTC 0162-1), Osaka, Japan, 13–18 November 2011.
10. Guo, H.; Jia, W.; Li, N. *Numerical and Experimental Investigation of Effect of Tongue Shape on Turbine Reliability*; SAE Technical Paper; No. 2018-01-0483; SAE: London, UK, 2018.
11. Yang, S.S.; Liu, H.L.; Kong, F.Y.; Xia, B.; Tan, L.W. Effects of the radial gap between impeller tips and volute tongue influencing the performance and pressure pulsations of pump as turbine. *J. Fluids Eng. Am. Soc. Mech. Eng. Digit. Collect.* **2014**, *136*, 5. [[CrossRef](#)]
12. Jin, J.M.; Jung, K.J.; Kim, Y.H.; Kim, Y.J. Effects of gap between impeller and volute tongue on a pressure fluctuation in double-suction pump. *J. Mech. Sci. Technol.* **2020**, *34*, 4897–4903. [[CrossRef](#)]
13. Wang, A.; Zheng, X. Design criterion for asymmetric twin-entry radial turbine for efficiency under steady and pulsating inlet conditions. *Proc. Inst. Mech. Eng. Part D J. Automob. Eng.* **2019**, *233*, 2246–2256. [[CrossRef](#)]
14. Ma, C.; Lu, K.; Li, W. The influence of a radial turbine volute on back-disk impingement cooling performance. *J. Braz. Soc. Mech. Sci. Eng.* **2020**, *42*, 446. [[CrossRef](#)]
15. Osipov, S.K.; Bylichkin, V.I.; Komarov, I.I.; Makhmutov, B.A. Podvodyashchij Patrubok Radialnoj Turbomashiny. Patent Rossiiskaia Federatsiia No. RU2749936C1, 6 June 2021.
16. Bardina, J.E.; Huang, P.G.; Coakley, T.J. Turbulence Modelling Validation. In Proceedings of the 28th Fluid Dynamics Conference, Reston, VA, USA, 29 June–2 July 1997.
17. Idelchik, I.E. *Handbook of Hydraulic Resistance*, 2nd ed.; Springer: Berlin/Heidelberg, Germany, 1986.
18. Cengel, Y.A.; Cimbala, J.M. *Fluid Mechanics: Fundamentals and Applications*; McGraw-Hill Higher Education: New York, NY, USA, 2013.